NASA Contractor Report 178112

(NASA-CR-178112) CRITERION FOR MIXED MODE FRACTURE IN COMPOSITE BONDED JOINTS Final Report (Missouri Univ.) 27 p EC A03/MF A01 CSCL 11D

N86-26380

Unclas
G3/24 43587

CRITERION FOR MIXED MODE FRACTURE IN COMPOSITE BONDED JOINTS

S. Mall and N. K. Kochhar

UNIVERSITY OF MISSOURI-ROLLA
ROLLA, MISSOURI

GRANT NAG1-425
May 1986

National Aeronautics and Space Administration

Langley Research Center
Hampton, Virginia 23665

ABSTRACT

A study was undertaken to characterize the debond growth mechanism of adhesively bonded composite joints under mode I, mixed mode I-II, and mode II static loadings. The bonded system consisted of graphite/epoxy (T300/5208) composite adherends bonded with a toughened epoxy (EC 3445) adhesive. The mode I, mode II and mixed-mode I-II fracture energies of the tested adhesive were found to be equal to each other. Furthermore, the criterion for mixed mode fracture in composite bonded joints was found to be: $(G_I/G_{IC}) + (G_{II}/G_{IIC}) = 1$.

INTRODUCTION

The adhesive bonding of laminated composite materials does not require that structural members being jointed be perforated to facilitate bolts. Without the bolt holes and stress concentrations associated with them, substantial weight savings can be realized which is a major reason for selecting composite materials for structural components. Adhesive joints usually fail by progressive crack growth and thus an appropriate failure criterion must be based upon the initiation and propagation of flaw inherent in the joint. Consequently, the fracture mechanics approach can be used to characterize their failure. Such an approach has been used to predict the failure of adhesively bonded joints (1-2).

The majority of this work has been concerned with the opening or cleavage mode failure (mode I). A crack in an isotropic medium will propagate in Mode I fracture regardless of the orientation of the initial flaw with respect to the applied stress. However, this is not necessarily the case in joint fracture since crack propagation is constrained to the adhesive layer regardless of the orientation of the adhesive layer, except, of course, when the substrate has a lower toughness than the adhesive. Thus, for structural design purposes, attention must be given to joint fracture under additional loading modes. Several studies were, therefore, undertaken to extend the applicability of the fracture mechanics approach for mode II (shear loading only) and mixed mode I-II (combination of tensile and

shear loading) fractures (1-2). As far as the authors are aware, all the above mentioned studies were concerned with adhesive bonds between metal adherends. Recently, a study has been reported involving the fracture behavior of a composite-adhesive-composite system under mode I condition only (3).

The objective of the present study was, therefore, to characterize the debond growth mechanism of adhesively bonded composite joints under mode I, mixed mode I-II, and mode II static loading. For this purpose, graphite/epoxy double-cantilever beam (DCB) specimens, cracked-lap-shear (CLS) specimens and end-notch flexure (ENF) specimens were tested using EC 3445 adhesive. This study focussed on the measuring of the critical strain-energy-release rates G_{IC}, $G_{(I-II)C}$ and G_{IIC} to determine the fracture mode dependence of debond failure.

TEST MATERIAL AND SPECIMEN CONFIGURATION

The debond system consisted of graphite/epoxy (T300/5208) adherends bonded with EC 3445 adhesive. The 3445 adhesive is a thermosetting paste with a cure temperature of 121°C. Specimens were fabricated by the conventional secondary bonding procedure. The bonding process followed the manufacturer's recommended procedure. The nominal adhesive thickness was 0.10 mm.

Three specimen types were fabricated: DCB, CLS and ENF specimens, as shown in Figures 1, 2 and 3. The DCB specimens were used to characterize debond growth under opening mode I loading (Fig 1) and also under mixed-mode loading (Fig 4). The CLS and ENF specimens were employed to study debond failure under mixed-mode I-II and sliding mode II loading, respectively.

The DCB specimen (Fig 1) consisted of two bonded adherends, each having 14 unidirectional plies with an initial debond length of 38 mm. This debond was introduced by a Teflon film of thickness equal to the adhesive bondline. Two aluminum end tabs were bonded to the DCB specimen to apply the load. The adherends of CLS specimens (Fig 2) consisted of quasi-isotropic lay-ups, $[0/45/-45/90]_S$ and $[0/45/-45/90]_{2S}$. Two configurations of CLS specimens were tested: 8-ply strap bonded to 16-ply lap and 16-ply strap bonded to 8-ply lap. The CLS specimen did not have an initial debond like the DCB specimen. The ENF specimens were obtained by bonding two composite adherends with an initial debond introduced by a Teflon film. These adherends were 15-ply unidirectional laminates.

TESTING PROCEDURE

The objective of the test program was to measure the critical strain-energy-release rates, G_{IC}, G_{IIC} and $G_{(I-II)C}$ for opening, shear and mixed-mode loadings, respectively. These are described separately in the following.

Mode I test

All static tests of DCB specimens were performed in a displacement controlled test machine. Prior to testing, these specimens were fatigued to create a debond of at least 6 mm beyond the end of the Teflon film. The test involved the application of displacement at a slow crosshead speed (5.0 mm/min). When the load reached the critical value, the debond grew in a stable manner. The onset of growth resulted in a deviation from linearity in the load versus

crosshead displacement record. The applied displacement was then decreased until a zero load reading was observed. After each static test, the specimen was fatigued until the debond grew at least 6 mm further, thus forming a sharp crack for the next static test. A series of static tests was performed on each specimen, which provided compliance and critical load measurements for several debond lengths. These measurements provided the critical strain-energy-release rate as explained in the section entitled 'ANALYSIS'.

Mode II test

Prior to testing, the ENF specimen was fatigued to create a debond of at least 6 mm beyond the end of Teflon film. This specimen was, then, loaded in three-point bending in a displacement controlled mode. The center point displacement and the corresponding load were recorded. The onset of debond growth resulted in a deviation from linearity in the load versus displacement record. The debond growth was stable in all tests. A clip-gage near the crack front was also used to measure accurately the critical load corresponding to the onset of debond growth. This confirmed further that debond growth occurred at the moment when there was a deviation from linearity in the load versus displacement (at the center) record. Two or more static tests were performed on each specimen. After each static test, the specimen was fatigued until the debond grew at least 6 mm further, thus forming a sharp crack for the next static test.

Mixed-mode test

The mixed-mode fracture tests were conducted with DCB and CLS specimens. This was accomplished with the DCB specimen by restraining the vertical motion of the uncracked end while loading only one end of the cracked end, as shown in Fig. 4. This procedure has been used to measure interlaminar toughness by Jordon and Bradley (4). For this purpose, a fixture was devised for the Instron testing machine. The test involved the application of displacement at a slow crosshead speed (5 mm/min). The debond grew in a stable manner and a corresponding critical load was recorded accurately with a clip-gage near the crack front.

Fracture tests with CLS specimens were conducted in a displacement-controlled mode. Prior to static testing, this specimen was fatigued, and thus it had an initial sharp debond. During the test, the axial load and displacement were recorded. The displacement was measured with two displacement transducers attached on the opposite sides of the specimen. The applied load was increased slowly until the debond propagated. The critical load corresponding to unstable debond growth was measured and verified by the deviation from linearity in the recorded load-displacement curve.

ANALYSIS

The measured data from the above mentioned four tests were analyzed differently to compute the critical strain-energy-release rates in each case. These are described separately in the following.

Mode I

The measured data provided the critical load, P_{cr}, and the compliance, C, for each debonded length, a, which were used to compute the fracture toughness. The details of this procedure are given in Reference 5. A compliance relationship of

$$C = A_1 a^3 \tag{1}$$

was fitted through the experimental data points by the method of least squares. This relationship, based on linear beam theory, fitted very well with the experimental data. The constant A_1 in Eq 1, from linear beam theory, is 2/3EI where E is the extensional stiffness and I is the second moment of area of each side of the DCB specimen. The experimental value of A_1 was in agreement with its counterpart obtained from the linear beam theory. Further, a finite element analysis of the DCB specimen was carried out (5). The FEM results were also in agreement with the measured compliance, as expressed by Eq 1, thus verifying the linear beam theory represents the appropriate behavior of the current DCB specimen. Based on the linear beam theory, a relationship of the form

$$P_{cr} = A_2/a \tag{2}$$

was fitted to the experimental data by the method of least squares. Then, the averaged value of G_{IC} for each specimen was computed from the relationship

$$G_{IC} = \frac{P_{cr}^2}{2w} \frac{\partial C}{\partial a} = 3A_1 A_2^2/(2w) \tag{3}$$

where w is the specimen width.

Mode II

The end-notched flexure tests have been developed to measure the interlaminar shear fracture toughness, G_{IIC}, of composite laminates (6). A closed-form equation to compute G_{II} was derived for this test using the linear beam theory. This analysis yielded the following expression of compliance, C and strain-energy-release rate G_{II},

$$C = \frac{2L^3 + 3a^3}{8Ebh^3} \tag{4}$$

$$G_{II} = \frac{9P^2a^2}{16b^2E\,h^3} \tag{5}$$

where P is the applied load, E is modulus, and a, b and h are as shown in Fig 2. However, in the present study, this test specimen was analyzed with a two-dimensional finite element program called GAMNAS (7) to evaluate its performance.

A finite element model, shown in Fig 5, consisted of 1000 isoparametric four-node elements and had about 2400 degrees of freedom. The adhesive was modeled with four layers of elements with the debond front at the middle of the adhesive layer. The element size in the vicinity of the crack front was 0.02 x 0.02 mm in order to evaluate accurately the strain-energy-release rate G_{II}. This size was selected by previous experience (5) as well as by conducting a convergence test on the G_{II} calculation with mesh refinement. The error in G_{II} obtained in the present study is

estimated to be less than ± 2 percent. The strain energy release rate, G_{II}, in the analysis was computed using a virtual crack closure technique (7). The plane strain condition was assumed in the finite element analysis.

The analysis indicated that mode II deformation is achieved at the crack tip and that the accompanying mode I deformation causes closure and overlapping of the opposite faces of the crack. This is not possible physically. To prevent the overlapping of crack faces, the nodal coupling technique, available with the GAMNAS program (7), was used. For this purpose, the multipoint constraint was applied at corresponding nodes to have the same displacements normal to the crack faces. This resulted in the pure mode II condition, i.e. $G_I = 0$.

Figure 6 shows the comparison of the measured compliance with FEM and the theoretical compliance (Eq 5). This clearly shows that the FEM results are in good agreement with the experimental values. Figure 7 shows the comparison of G_{II} obtained from FEM analysis and from a linear beam theory, i.e. Eq 5. In the present study, G_{IIC} was computed from the FEM analysis, since the theoretical expressions (Eqs 4 & 5) were not developed for the bonded ENF specimen.

Mixed mode I-II

The tested CLS specimens were analyzed with the finite element program GAMNAS (7) to compute G_I and G_{II} for a given geometry, debond length and applied load. This two-dimensional analysis accounted for the geometric nonlinearity associated with large rotation in these specimens. The details of the FEM analsis of CLS specimens have been reported in Reference 8.

Jordon and Bradley (4) have developed the following relationships based on the linear beam theory to compute G_I and G_{II} associated with interlaminar crack growth of composite laminate from an asymmetrically loaded DCB specimen as shown in Fig 4.

$$G_I = \frac{P^2 a^2}{4wEI} \tag{6}$$

$$G_{II} = \frac{3P^2 a^2}{16wEI} \tag{7}$$

In the present study, geometrically nonlinear FEM analysis of this specimen was, however, conducted to evaluate its performance for bonded systems, and to account for its nonlinear behavior due to large deflections.

DEBOND MECHANISM

In all the fracture tests, the debond growth occurred in a cohesive manner, i.e. it grew within the adhesive. This growth remained in the bondline during the mode I and mode II tests with DCB and ENF specimens, respectively. However, during the mixed mode test with both DCB and CLS, the debond propagated into the composite adherend after its cohesive initiation in the adhesive.

RESULTS AND DISCUSSIONS

The critical strain-energy-release rates, G_{IC}, G_{IIC}, $G_{(I-II)C}$ and G_I/G_{II} obtained from all the specimens tested are summarized in Tables 1-4. The observed variation in G_{IC}, G_{IIC} and $G_{(I-II)C}$ is

reasonable as compared to other mechanical properties of adhesives as well as with previous studies (1-2).

The difference in G_{IIC} obtained from FEM analysis and Eq 5, as given in Table 2, shows that the closed-form expression derived for delamination studies (6) does not represent the appropriate behavior of the bonded system. The same observation should also be noted for $G_{(I-II)C}$ obtained from the DCB as given in Table 4. The values of G_{IIC} and $G_{(I-II)C}$ from FEM analysis in Tables 2 and 4 will be, therefore, considered in the following.

To show the interaction between fracture modes I and II, experimental data from all the specimens are plotted in Fig 8. The data in Fig 8 define the functional relationship between G_I and G_{II} for the debond growth in the presence of tensile and in-plane shear stresses. This mixed-mode interaction is usually expressed in the fracture mechanics literature as

$$\left\{\frac{G_I}{G_{IC}}\right\}^m + \left\{\frac{G_{II}}{G_{IIC}}\right\}^n = 1 \qquad (8)$$

Therefore, the present data have been replotted in Fig 9 using the average values of G_{IC} and G_{IIC}. These show the following linear relationship for mixed mode debond growth in EC 3445 adhesive.

$$\frac{G_I}{G_{IC}} + \frac{G_{II}}{G_{IIC}} = 1 \qquad (9)$$

A previous study (9) has shown that fracture energy increased by introducing a mode II component in the unmodified epoxy adhesive

(DGEBA-TEPA). For this unmodified epoxy adhesive, G_{IIC} was about an order of magnitude larger than G_{IC}. On the other hand, the toughened epoxy adhesive (DGEBA-CTEN-PIP) exhibited complex behavior. The mixed mode $G_{(I-II)C}$ values were significantly lower than the mode I or mode II values with these latter two fracture energies equal in magnitude. This decrease in mixed mode values was attributed to the interfacial failure. The EC 3445 adhesive is a structural rubber toughened epoxy adhesive. The results of the present study with EC 3445 are in agreement with the previous study (9) for mode I and mode II loading, i.e. G_{IC} and G_{IIC} are equal to each other for all practical purposes. Further, the mixed mode fracture toughness, $G_{(I-II)C}$, for a wide range of G_I and G_{II} ratios, was also found equal to G_{IC} and G_{IIC} in the present adhesive, for all practical purposes. This can be attributed to the cohesive failure of the bondline in the mixed mode loading in the present study, unlike the previous study (9) where it occurred adhesively.

CONCLUSIONS

A combined experimental-analytical investigation of composite-to-composite bonded joints was undertaken to characterize the mechanics of debond growth. The system studied consisted of graphite/epoxy adherends bonded with EC 3445 adhesive. Several types of specimens were tested which provided the critical strain-energy-release rates G_{IC}, G_{IIC} and $G_{(I-II)C}$ under various load conditions: mode I loading, mode II loading and mixed mode I-II loading. This study led to the following conclusions:

(a) The mode I, mode II and mixed mode I-II fracture energies of the toughened epoxy adhesive are equal to each other.

(b) The fracture criterion for the mixed mode fracture of the toughened epoxy adhesive can be expressed as:

$$\frac{G_I}{G_{IC}} + \frac{G_{II}}{G_{IIC}} = 1$$

ACKNOWLEDGEMENT

The work reported here was supported by NASA Langley Research Center, Hampton, VA. The authors wish to acknowledge the support and encouragement of Dr. W. S. Johnson, NASA Langley Research Center during the course of this investigation.

REFERENCES

1. Kinloch, A.J. Review-the science of adhesion--part 2, mechanics and mechanisms of failure. Journal of Material Science, 1982, 17, 617-651.

2. Shaw, S.J. Adhesion 7, Applied Science Publishers, 1982, 173-196.

3. Ripling, E.J., Satner, J.C., and Crosley, P.B. Fracture of composite-adhesive-composite systems. Adhesive Joints: Their Formation, Characteristics, and Testing, Plenum Press, 1984.

4. Jordon, W.M. and Bradley, W.L. Micromechanics of fracture in toughened graphite-epoxy laminates. Toughened Composites, ASTM STP 937, American Society for Testing and Materials, 1987 (in press).

5. Mall, S. and Johnson, W.S. Characterization of mode I and mixed-mode failure of adhesive bonds between composite adherends. NASA Technical Memorandum 86355, 1985.

6. Russell, A.J. and Street, K.N. Factors affecting the interlaminar fracture energy of graphite/epoxy laminates. Progress in Science and Engineering of Composites, Proc. ICCM-IV, Japan Society for Composite Materials, 1982.

7. Dattaguru, B., Everett, R.A., Jr., Whitcomb, J.D., and Johnson, W.S. Geometrically-Nonlinear analysis of adhesively bonded joints. Journal of Engineering Materials and Technology, ASME, 106, 59-65.

8. Mall, S., Johnson, W.S., and Everett, R.A., Jr. Cyclic debonding of adhesively bonded composites. Adhesive Joints: Their Formation, Characteristics, and Testing, Plenum Press, 1984.

9. Bascom, W.D. and Oroshnik, J. Effect of bond angle on mixed-mode adhesive fracture. Journal of Material Science, 1978, 13, 1411-1418.

Table 1. G_{IC} from DCB specimens

Specimen No.	1	2	3	4	5	6	Avg.
G_{IC}, J/m^2	810	860	878	906	920	952	888

Table 2. G_{IIC} from ENF specimens

Specimen No.	a/L	G_{IIC}, J/m^2	
		FEM	Eq 5
1	0.5	929	707
1	0.625	945	803
1	0.75	908	742
2	0.5	952	722
2	0.625	858	730
2	0.75	844	690
3	0.5	1022	778
3	0.625	900	767
3	0.75	824	673
	Avg.	909	734

Table 3. $G_{(I-II)C}$ from CLS specimens

Specimen No.	Strap Plies / Lap Plies	$\frac{G_I}{G_{II}}$	$G_{(I-II)C}$ J/m^2	Avg. $G_{(I-II)C}$ J/m^2
1	16/8	0.31	910	
2	16/8	0.31	870	858
3	16/8	0.31	795	
4	8/16	0.25	840	
5	8/16	0.25	790	838
6	8/16	0.25	885	

Table 4. $G_{(I-II)C}$ from DCB specimens

Specimen No.	$\frac{a}{L}$	G_I/G_{II}	$G_{(I-II)C}$, J/m^2	
			FEM	Eqs 6 & 7
1	0.813	1.24	963	1053
2	0.925	1.24	998	1165
3	0.925	1.24	936	1032
		Avg.	965	1083

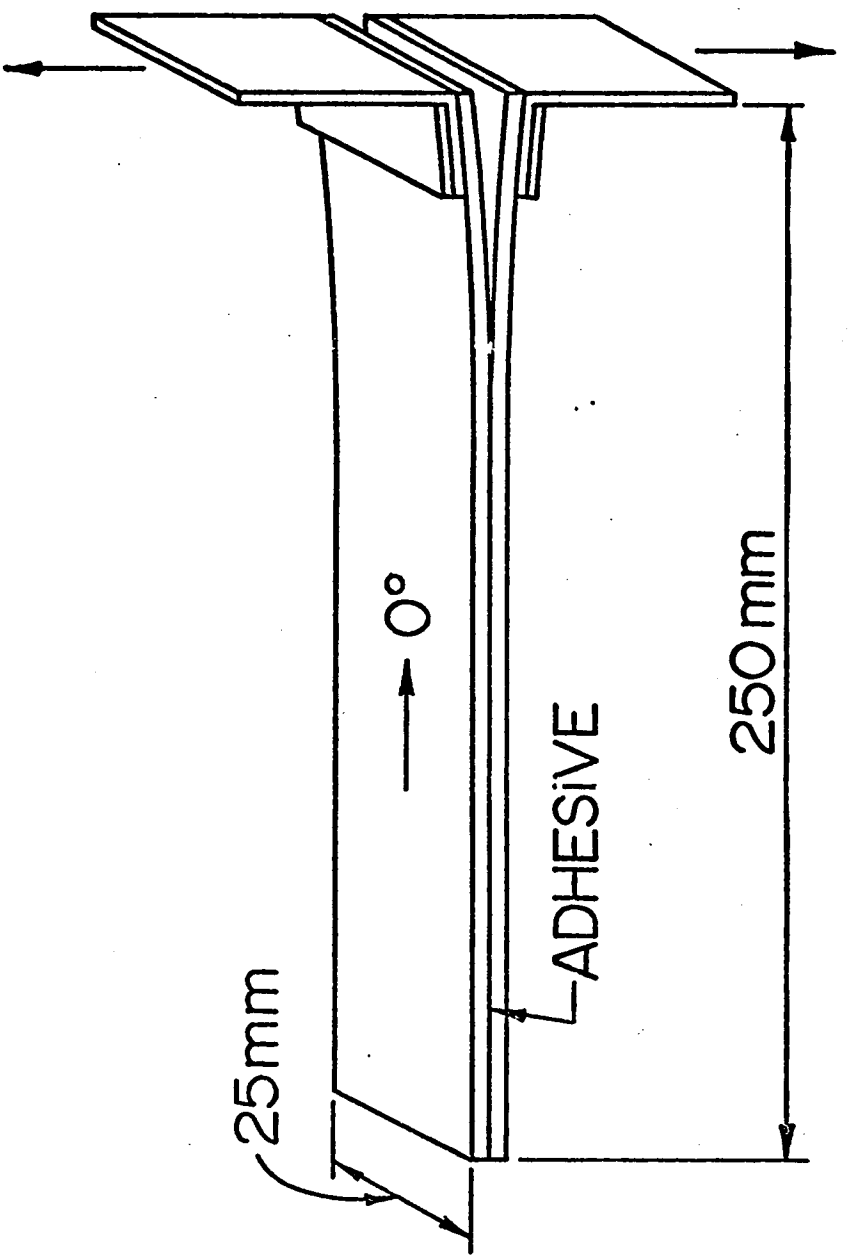

Figure 1. Double-cantilever beam specimen

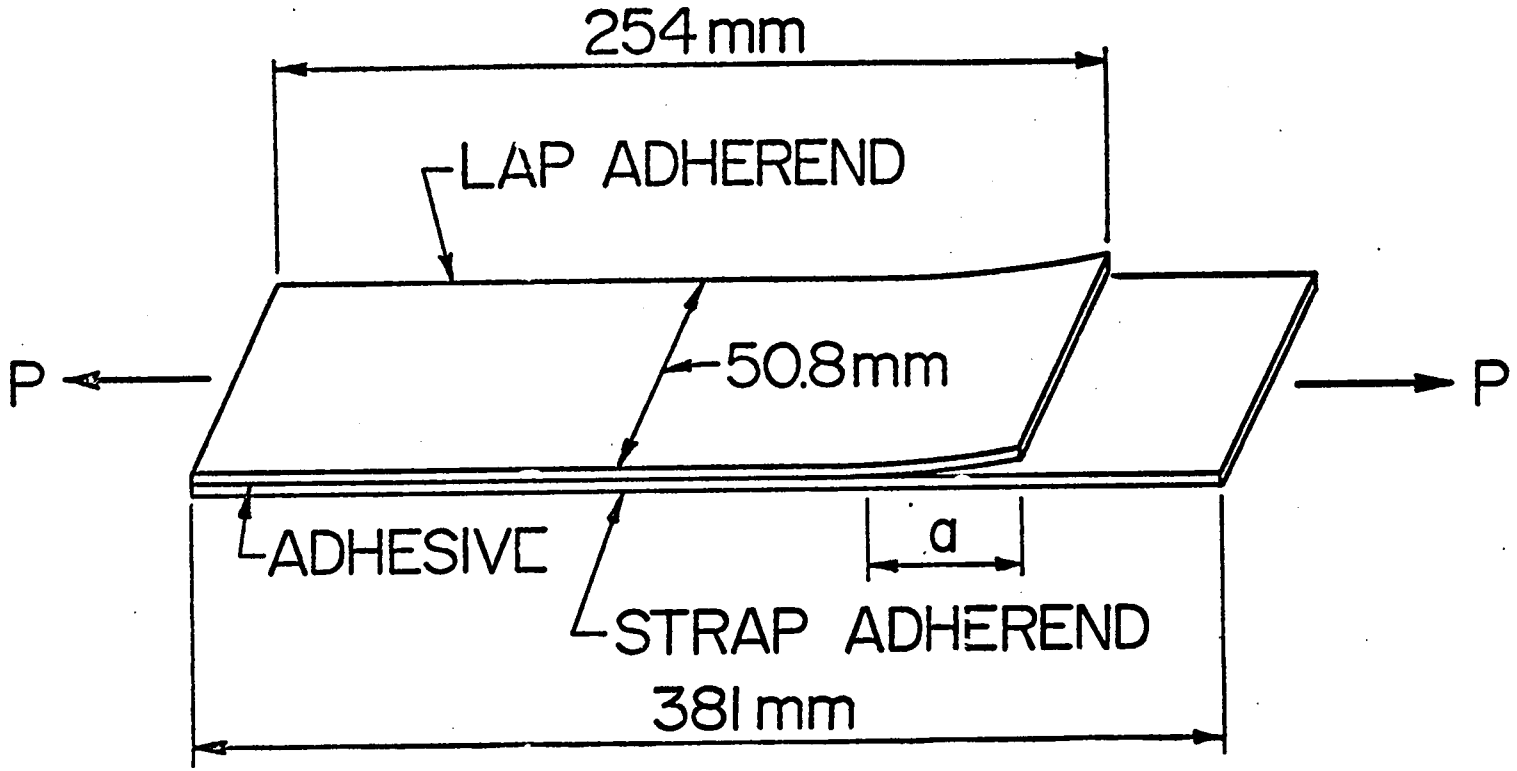

Figure 2. Cracked-lap-shear specimen

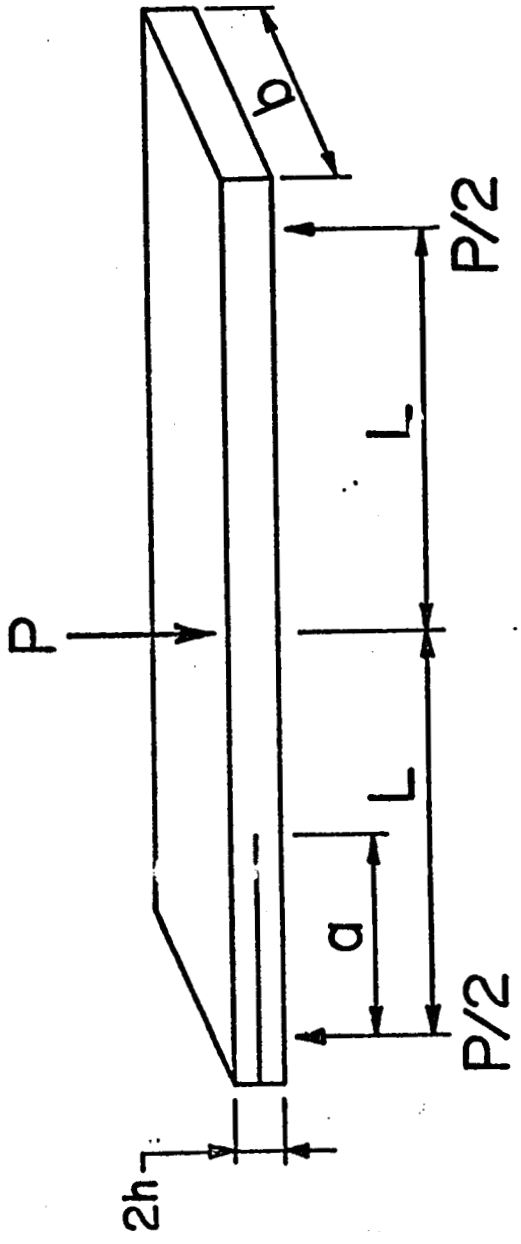

Figure 3. End-notched flexure specimen (L = 50.8 mm, 2h = 4 mm, b = 25.4 mm)

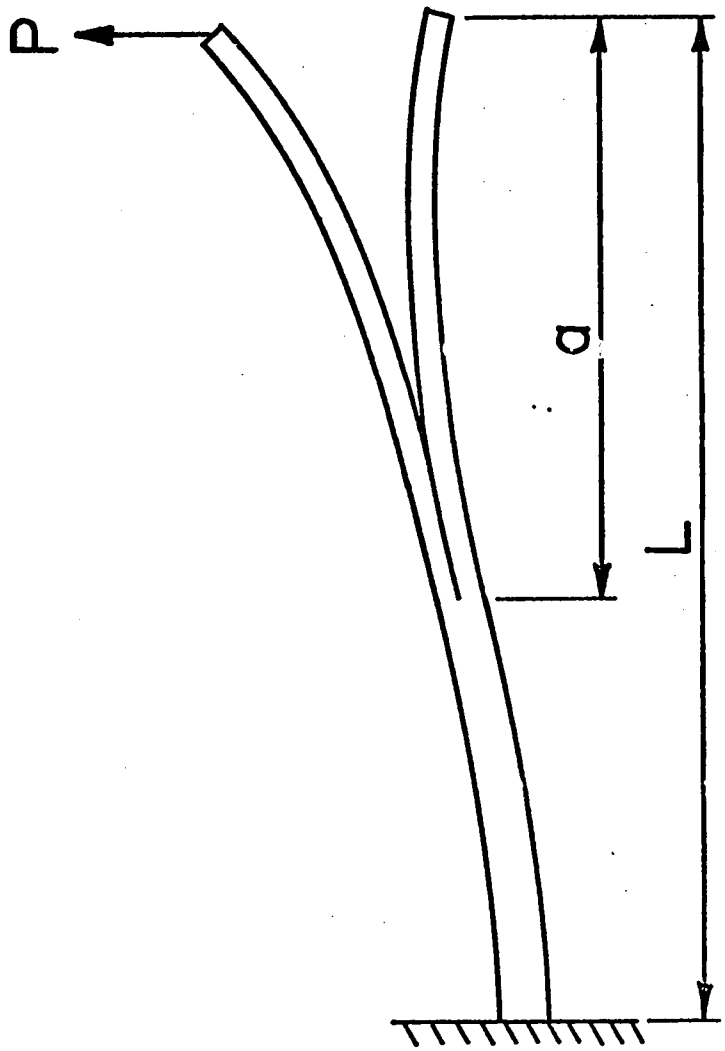

Figure 4. Asymmetrically loaded double-cantilever beam specimen (L = 203 mm)

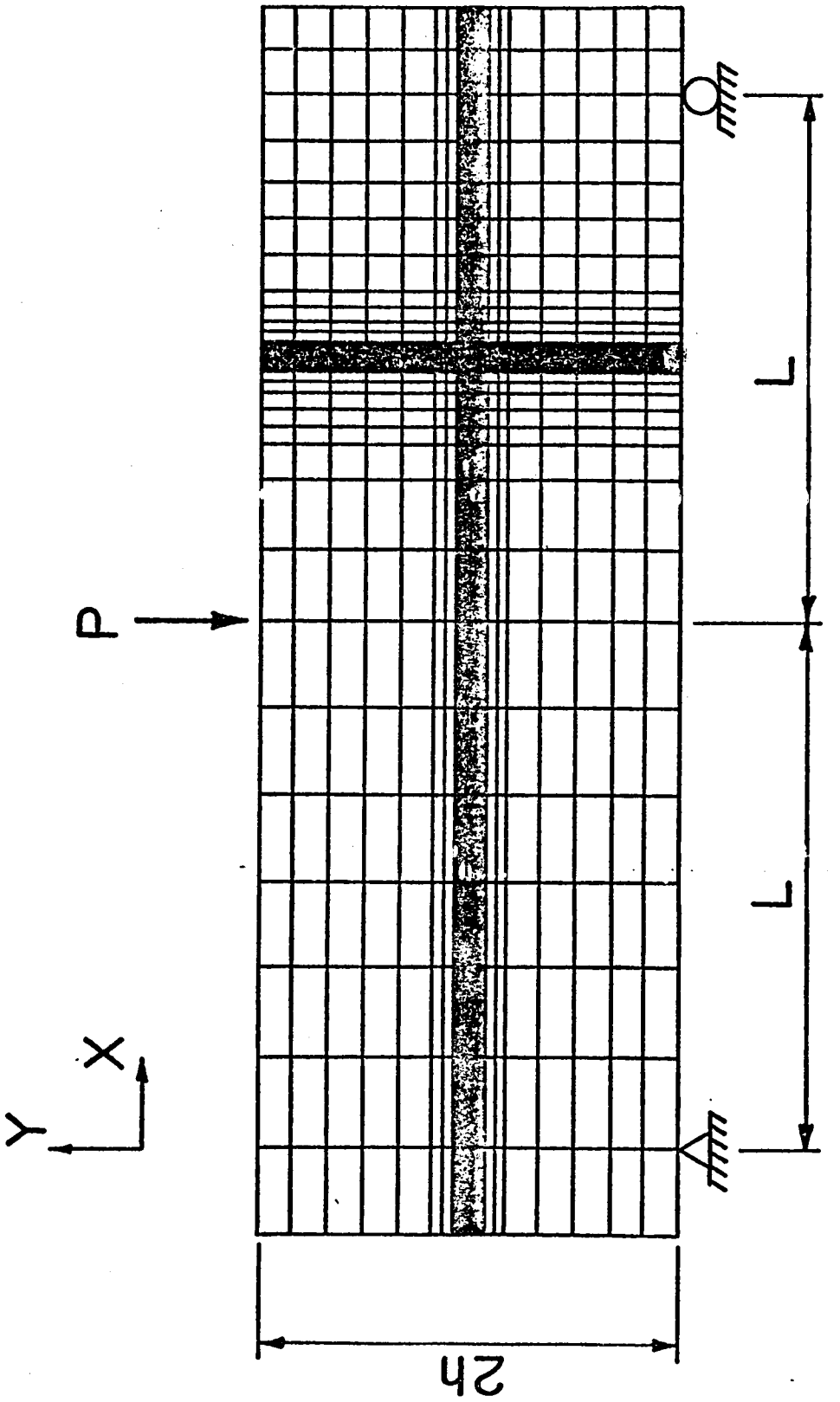

Figure 5. Finite element mesh (y coordinates are magnified 10x)

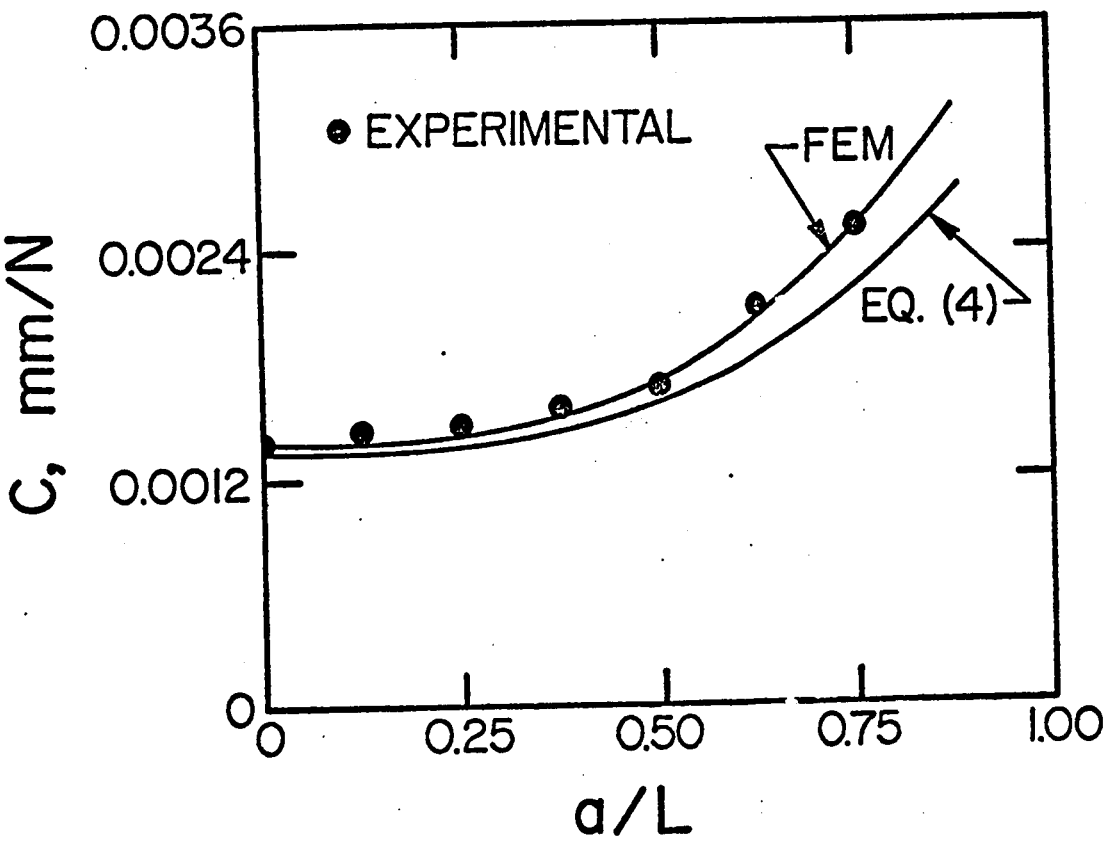

Figure 6. Relation between compliance, C, and normalized crack length, a/L, of ENF specimen

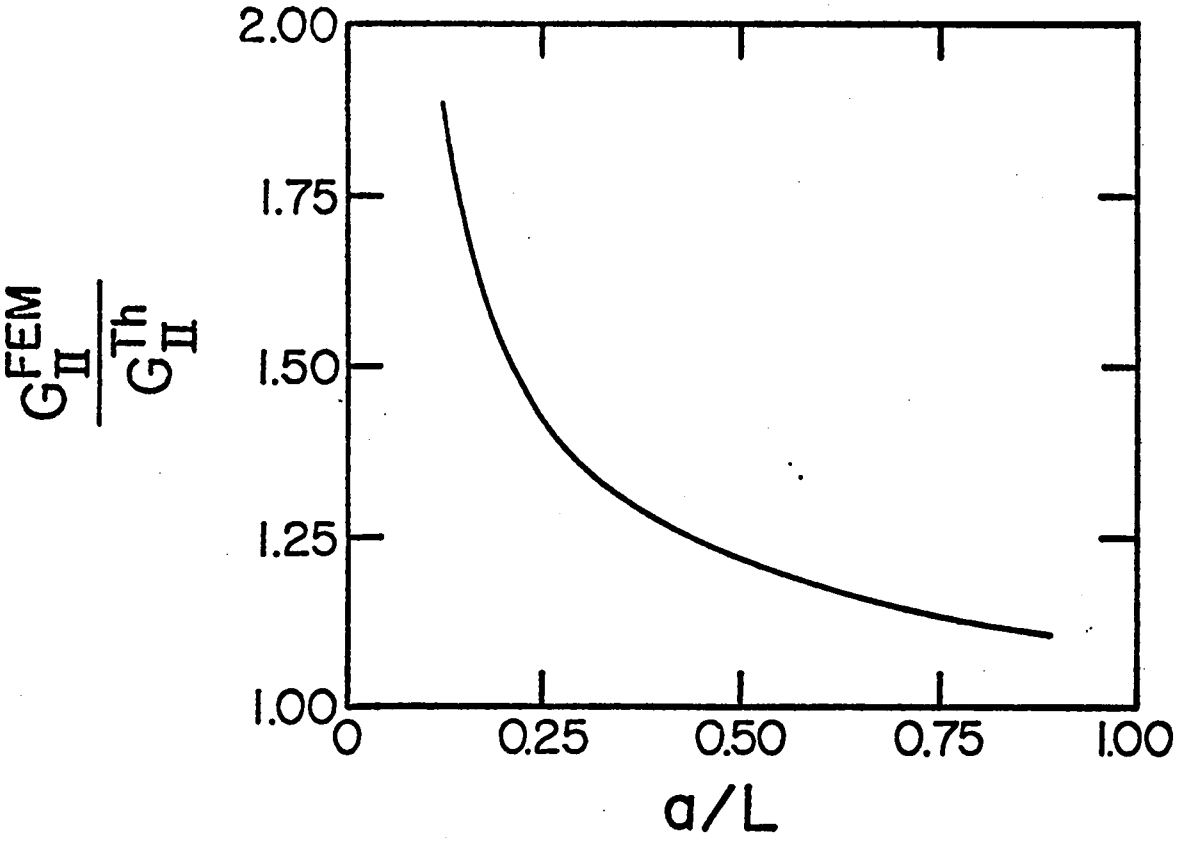

Figure 7. Ratio of strain-energy-release rate from FEM analysis, G_{II}^{FEM}, and from Eq 5, $G_{I.I}^{Th}$, as a function of normalized crack length, a/L, for ENF specimens

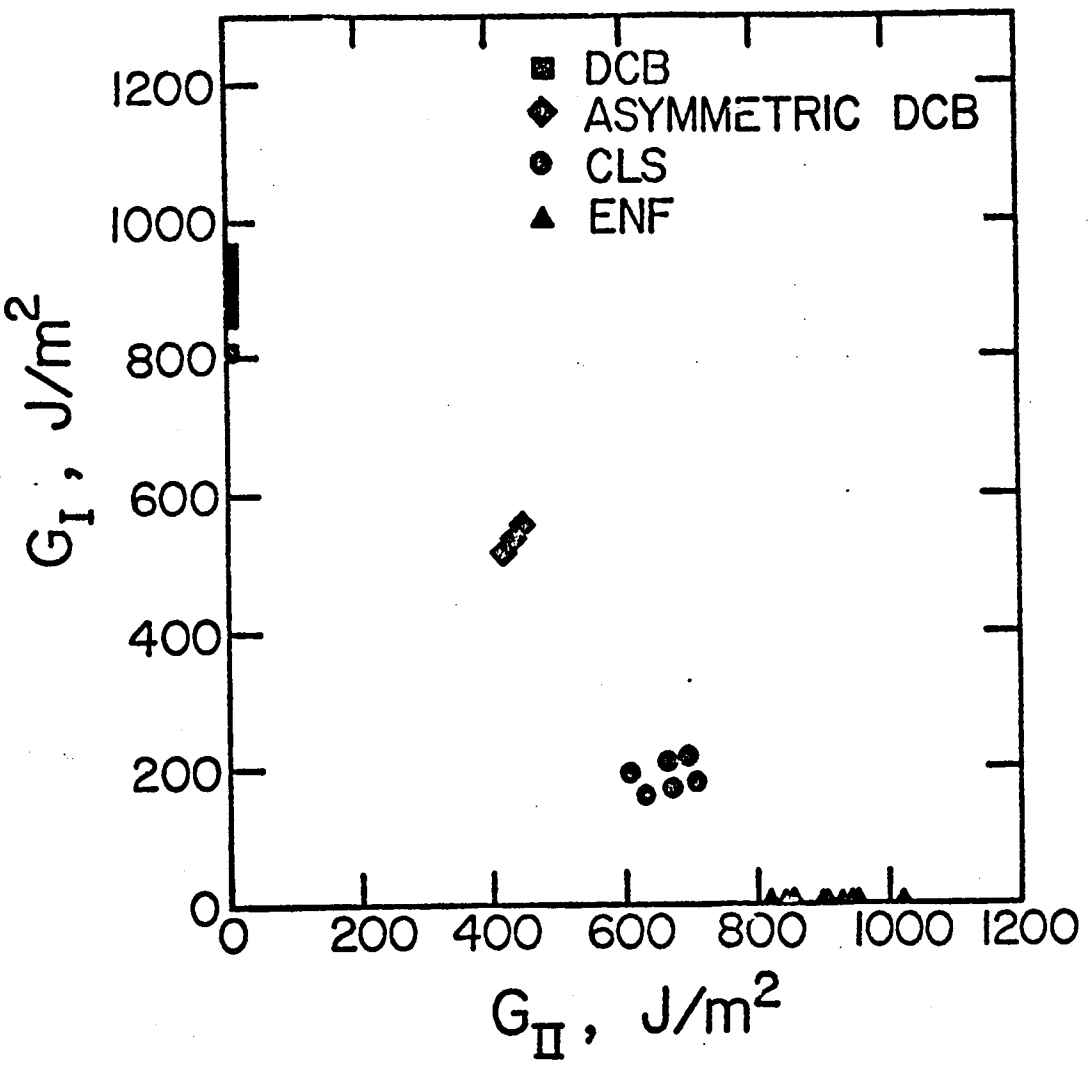

Figure 8. Interaction between G_I and G_{II}

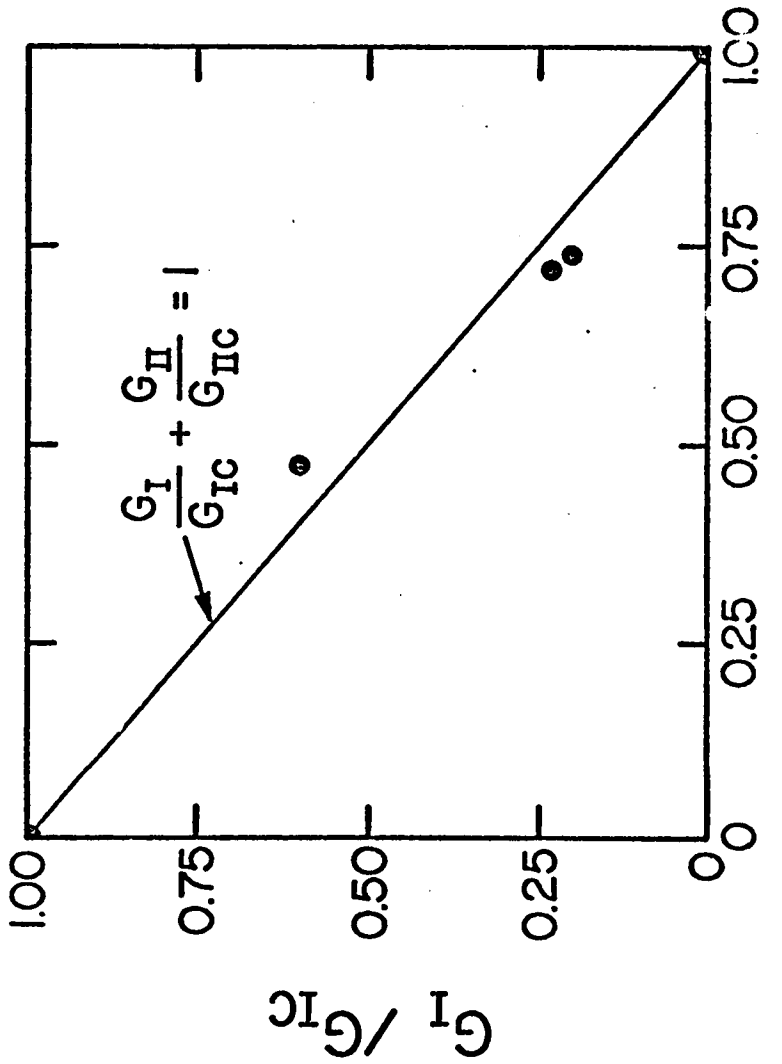

Figure 9. Relationship between G_I/G_{IC} and G_{II}/G_{IIC}

Standard Bibliographic Page

1. Report No.	2. Government Accession No.	3. Recipient's Catalog No.
NASA CR-178112		

4. Title and Subtitle	5. Report Date
CRITERION FOR MIXED MODE FRACTURE IN COMPOSITE BONDED JOINTS	May 1986
	6. Performing Organization Code
7. Author(s)	8. Performing Organization Report No.
S. Mall and N. K. Kochhar	
9. Performing Organization Name and Address	10. Work Unit No.
University of Missouri-Rolla Department of Engineering Mechanics M-394-3516 Rolla, MO 05401	11. Contract or Grant No. NAG1-425
12. Sponsoring Agency Name and Address	13. Type of Report and Period Covered Contractor Report
National Aeronautics and Space Administration Washington, DC 20546	14. Sponsoring Agency Code 534-06-23-03

15. Supplementary Notes

Langley Technical Monitor: Dr. W. S. Johnson
Final Report

16. Abstract

A study was undertaken to characterize the debond growth mechanism of adhesively bonded composite joints under mode I, mixed mode I-II, and mode II static loadings. The bonded system consisted of graphite/epoxy (T300/5208) composite adherends bonded with a toughened epoxy (EC 3445) adhesive. The mode I, mode II and mixed-mode I-II fracture energies of the tested adhesive were found to be equal to each other. Furthermore, the criterion for mixed mode fracture in composite bonded joints was found to be: $(G_I/G_{IC}) + (G_{II}/G_{IIC}) = 1$.

17. Key Words (Suggested by Authors(s))	18. Distribution Statement
Debond growth mechanism Adhesively bonded composite joints Graphite/epoxy Mixed mode fracture Composite bonded joints	Unclassified-Unlimited Subject Category 24

19. Security Classif.(of this report)	20. Security Classif.(of this page)	21. No. of Pages	22. Price
Unclassified	Unclassified	26	A03

For sale by the National Technical Information Service, Springfield, Virginia 22161